© 2017. Published by The Company of Biologists Ltd | Journal of Cell Science (2017) 130, 3588-3600 doi:10.1242/jcs.204461

RESEARCH ARTICLE

Association of FK506 binding proteins with RyR channels – effect of CLIC2 binding on sub-conductance opening and FKBP binding

Spencer J. Richardson[1,*], Gregory A. Steele[2,*], Esther M. Gallant[1], Alexander Lam[3], Charles E. Schwartz[4], Philip G. Board[1], Marco G. Casarotto[1], Nicole A. Beard[5] and Angela F. Dulhunty[1,‡]

ABSTRACT

Ryanodine receptor (RyR) Ca^{2+} channels are central to striated muscle function and influence signalling in neurons and other cell types. Beneficially low RyR activity and maximum conductance opening may be stabilised when RyRs bind to FK506 binding proteins (FKBPs) and destabilised by FKBP dissociation, with submaximal opening during RyR hyperactivity associated with myopathies and neurological disorders. However, the correlation with submaximal opening is debated and quantitative evidence is lacking. Here, we have measured altered FKBP binding to RyRs and submaximal activity with addition of wild-type (WT) CLIC2, an inhibitory RyR ligand, or its H101Q mutant that hyperactivates RyRs, which probably causes cardiac and intellectual abnormalities. The proportion of sub-conductance opening increases with WT and H101Q CLIC2 and is correlated with reduced FKBP–RyR association. The sub-conductance opening reduces RyR currents in the presence of WT CLIC2. In contrast, sub-conductance openings contribute to excess RyR 'leak' with H101Q CLIC2. There are significant FKBP and RyR isoform-specific actions of CLIC2, rapamycin and FK506 on FKBP–RyR association. The results show that FKBPs do influence RyR gating and would contribute to excess Ca^{2+} release in this CLIC2 RyR channelopathy.

KEY WORDS: Ryanodine receptor, FKBP12 and FKBP12.6, Sub-state opening, CLIC2, RyR channelopathy, FK506

INTRODUCTION

The RyR ion channel releases Ca^{2+} from sarcoplasmic reticulum (SR) and endoplasmic reticulum (ER) Ca^{2+} stores and is essential for excitation–contraction coupling in skeletal muscle and the heart. The main RyR isoforms expressed in skeletal muscle and in the heart are RyR1 and RyR2, respectively. RyR3 is expressed alone or with RyR1 and/or RyR2 in a variety of tissues and in many areas of the brain (Dulhunty et al., 2011). The >2 MDa RyR homotetramer, with its associated proteins, forms a Ca^{2+}-signalling complex that extends from the SR lumen through the cytoplasm to the extracellular space. It is regulated by numerous cytosolic factors including the 12 kDa and 12.6 kDa binding proteins (FKBP12 and FKBP12.6) for the immunosuppressant drug FK506 (Lanner et al., 2010). FKBP12 alone is expressed in skeletal muscle and binds to RyR1, whereas FKBP12 and FKBP12.6 are expressed in the heart and central nervous system in most species, and both are bound to RyR2 (Lanner et al., 2010). Structural analysis of RyRs shows a 'clamp' region that contains important regulatory sites, including the FKBP12 or FKBP12.6 binding site (Samsó et al., 2006; Yan et al., 2015). The association of FKBPs with RyRs impacts channel gating mechanisms and disruption of this interactions has been implicated in Ca^{2+} mishandling that underlies many cardiac and skeletal myopathies (Chelu et al., 2004; Bellinger et al., 2008).

The nature of the regulation of RyRs by FKBPs is unclear. There is evidence that FKBPs stabilize channel opening to the full conductance, reducing sub-conductance (sub-state) opening (Ahern et al., 1997; Marx et al., 1998; Mei et al., 2013). Others report that FKBPs do not impact channel conductance levels (Galfré et al., 2012; Xiao et al., 2007). These contradictions may, in part, be due to a lack of quantification of sub-state activity and a consistent definition of a sub-state opening. In general, low conductance openings lasting several seconds are considered to be sub-state events (Tripathy et al., 1998; Dulhunty et al., 2004; Smith et al., 2013), whereas similar briefer events are mainly ignored, although frequent low conductance events can contribute substantially to current flow from the SR. There is additional debate about the role of FKBPs and sub-state activity in muscle and brain disorders. In Ca^{2+}-release-based arrhythmias, FKBP bound to RyR2 channels has been found to be depleted in some studies (Wehrens et al., 2005; Györke and Carnes, 2008), but unaffected in other reports (Xiao et al., 2007; Zissimopoulos and Lai, 2009; Oda et al., 2015). There are also reports that FKBP12 binding to RyR1 is reduced in skeletal muscle weakness (Reiken et al., 2003; Rullman et al., 2013), and FKBP dissociation from RyRs is associated with seizures, cognitive dysfunction, and deficits in learning and memory (Lehnart et al., 2008; Liu et al., 2012b; Yuan et al., 2016).

In addition to the likely contribution of low conductance opening to Ca^{2+} release in Ca^{2+}-signalling disorders, the poorly understood mechanism underlying sub-state opening is important in that it provides a window into the gating mechanisms impinging on the RyR pore. Sub-state opening is reported in a number of different situations in addition to exposure to compounds considered to deplete FKBP bound to RyRs. These include exposure to scorpion toxins (Tripathy et al., 1998; Dulhunty et al., 2004; Smith et al., 2013) and the basic DHPR II–III loop peptide A (Dulhunty et al., 1999; Chen et al., 2003). This may suggest either that sub-state activity is a non-specific response to a variety of factors or that some, if not all, of the factors that induce sub-state activity do so by dissociating FKBPs from the RyRs. This second possibility is supported by our finding that peptide A induces sub-state activity if

[1]Eccles Institute of Neuroscience, John Curtin School of Medical Research, Australian National University, PO Box 334, ACT 2601, Australia. [2]Capital Pathology Laboratory, 70 Kent St, Deakin, ACT 2600, Australia. [3]Neurosurgery, Royal Perth Hospital, 197 Wellington St, Perth, WA 6000, Australia. [4]JC Self Research Institute, Greenwood Genetic Center, Greenwood, SC 29646, USA. [5]Cardiac Physiology Department, Health Research Institute, Faculty of Education Science and Mathematics, University of Canberra, Bruce, ACT 2617, Australia.
*These authors contributed equally to this work

‡Author for correspondence (angela.dulhunty@anu.edu.au)

G.A.S., 0000-0002-3948-1409; A.L., 0000-0001-7734-0087; P.G.B., 0000-0003-2752-0332; M.G.C., 0000-0002-0571-7671; N.A.B., 0000-0002-8212-2209; A.F.D., 0000-0001-9493-4944

Received 30 March 2017; Accepted 31 July 2017

Journal of Cell Science

Journal of Cell Science (2017) 130, 3588-3600 doi:10.1242/jcs.204461

added alone to native RyR1 channels, but not if FKBP12 is first removed by rapamycin (Dulhunty et al., 1999).

Sub-state activity is also observed when CLIC2 (type 2 Cl^- intracellular channel) binds to RyR channels (Board et al., 2004; Jalilian et al., 2008). CLIC2 is a soluble cytoplasmic protein at a cellular pH, but can form a chloride channel under very acidic pH conditions (Board et al., 2004; Dulhunty et al., 2005; Cromer et al., 2007; Jalilian et al., 2008). Wild-type (WT) CLIC2 inhibits RyR1 and RyR2 channels (Board et al., 2004; Dulhunty et al., 2005). An H101Q mutation in CLIC2, associated with intellectual deficit and cardiac dysfunction, also binds to RyRs, and produces hyperactive RyRs (Takano et al., 2012). The sub-state activity induced by binding of WT and H101Q CLIC2 to RyR channels has been reported but has not previously been measured and its effect on FKBP binding to RyRs is not known. Our aim here was to explore the increase in sub-state activity induced by WT and H101Q CLIC2 and determine whether this is correlated with FKBP binding under normal pH conditions that exist in the cytosol in the vicinity of RyR channels. To achieve this aim, a novel paradigm for quantifying RyR sub-state activity has been developed.

We show that the fraction of sub-state openings is significantly increased after exposure to WT and H101Q CLIC2. Both WT and H101Q CLIC2 deplete FKBP12 and FKBP12.6 bound to RyR2, and FKBP12 bound to RyR1. This is the first report that association of FKBP with RyRs can be reduced by factors that decrease channel activity. We demonstrate that the ability of compounds to dissociate FKBP from RyRs is strongly dependent on the isoforms of both proteins – a finding that may resolve some of the debate related to the effects of FKBPs on RyRs. The results support the hypothesis that sub-state gating with de-stabilization of channel opening to the full conductance can be indicative of reduced FKBP binding.

RESULTS

Sub-state opening induced by WT CLIC2 and H101Q CLIC2

We previously reported that WT CLIC2 inhibits RyR1 and RyR2 channels and that the H101Q mutation in CLIC2 reverses the effect of the WT protein, causing channel hyperactivity (Takano et al., 2012). The response of RyR1 and RyR2 channels to CLIC2 is saturated at concentrations between 2 and 4 µM CLIC2 (Board et al., 2004). RyR responses to 4 µM CLIC2 are examined here, unless otherwise stated. In Fig. 1A,B, it is clear that the effect of cytoplasmic addition of 4 µM WT CLIC2 was to reduce the number of channel open events and that most of the remaining openings were to levels less than the maximum open level (o). One or two dominant sub-state levels in these particular records are labelled (s). In contrast to results with WT CLIC2, addition of 4 µM H101Q CLIC2 increased the number of channel open events, particularly to low current levels (Fig. 1C,D). This increase in sub-state activity was seen in all channels, with openings to levels that were generally between 30% and 70% of the maximum single channel conductance. It is notable that, although the amplitude of levels varied from time to time in individual channels as well as between channels, both WT and H101Q CLIC2 enhanced the fraction of openings to these levels, irrespective of whether overall channel activity fell (WT) or increased (H101Q). In addition, the enhanced sub-state activity was independent of whether the channel activity was initially high (Fig. 1B) or relatively low (Fig. 1D) and was apparent at −40 mV (Fig. 1A,B,D) and +40 mV (Fig. 1C).

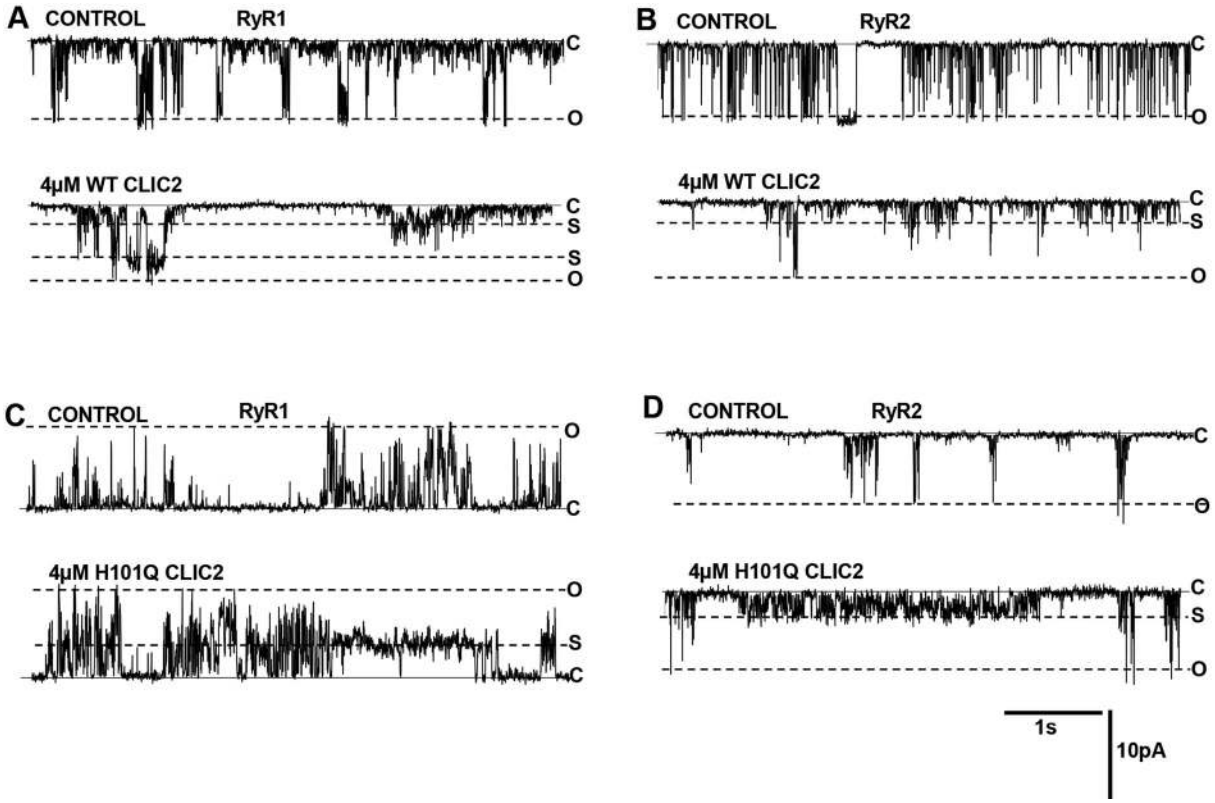

Fig. 1. WT and H101Q CLIC-2 induce sub-state activity in single RyR channels. (A-D) Five-second segments of representative single channel currents recorded before (top trace) and 3-5 min after (bottom trace) addition of the indicated CLIC2 construct. Currents recorded at –40 mV are shown in A,B,D, and at +40 mV in C, with channel opening from the closed level (c) to the maximum single channel current level (o) and to dominant sub-state levels (s) indicated by broken lines. WT CLIC2 was added to RyR1 in A and to RyR2 in B. H101Q CLIC2 was added to RyR2 in D and to RyR1 in C.

Journal of Cell Science (2017) 130, 3588-3600 doi:10.1242/jcs.204461

Since the H101Q CLIC2 mutation is associated with intellectual as well as cardiac abnormality (Takano et al., 2012), we examined its effect on brain RyRs. Again, 2-4 µM H101Q CLIC2 increased activity, with dominant sub-state openings (Fig. S1A) in 4 of 4 channels. We attempted to identify the brain RyR isoform using the peptide GSTM2C H5-8, a C-terminal fragment of the muscle-specific glutathione transferase (GSTM2). GSTM2C H5-8 specifically inhibits RyR2, but not RyR1 (Hewawasam et al., 2010), by binding to divergent region three of RyR2 (which has little sequence homology with RyR1 or RyR3) (Liu et al., 2012a). The brain RyRs failed to respond to 8 µM GSTM2C added after 2 µM H101Q CLIC2, suggesting that the channels were not RyR2. However, GSTM2C also failed to alter activity in 4 of 4 sheep heart RyR2 channels following their activation by 4 µM H101Q CLIC2 (Fig. S1). This lack of an effect might be explained if both H101Q CLIC2 and GSTM2C impinge on the same RyR2 gating mechanism; indeed, GSTM2C enhances sheep heart RyR2 sub-state activity (Samarasinghe et al., 2015), even though the GSTM2C binding D3 region of RyR2 is distinctly different from the CLIC2 binding site (Meng et al., 2009). The identity of the brain isoforms was not explored further. However, it is worth noting the brain RyRs were activated by H101Q CLIC2, in the same way as muscle RyR1 and RyR2, despite the lack of muscle-specific regulatory proteins that might influence the response to the mutant CLIC2. It is also worth noting that, although the RyR isoform involved in intellectual capacity is not yet identified, RyR1 and RyR2 are the major isoforms in the brain (Furuichi et al., 1994) and are similarly activated by H101Q CLIC2.

Definition of sub-state activity and quantification of the fraction of channel open probability attributable to sub-state openings

Current records with a total duration of ∼150 s were filtered at 200 Hz (as in records in Fig. 1) to better define open levels in the inherently noisy currents across bilayers with diameters of ∼100 µm. The amplitude of every open event is plotted against its duration in Fig. 2. Events of <4.5 ms were likely to be truncated by the 200 Hz filter and these events were excluded from the analysis. All events longer than 4.5 ms, with amplitudes between 10% and 90% of the maximum conductance were defined as sub-state openings. Specific levels were not defined as there is a continuum of levels as previously reported (Ahern et al., 1994, 1997; Jalilian et al., 2008).

It is notable, in Figs 1 and 2, that sub-state openings are present in control records from native channels not exposed to CLIC2, as noted previously (Ahern et al., 1994, 1997; Jalilian et al., 2008). However, there are more low-amplitude events after adding both WT and H101Q CLIC2 (Fig. 2, blue circles) than control (Fig. 2, black circles), and there is clustering of the openings (blue symbols) towards the −2pA level at −40 mV (Fig. 2A,B,D), or towards 2pA at +40 mV (Fig. 2C). The number of openings was less than in the

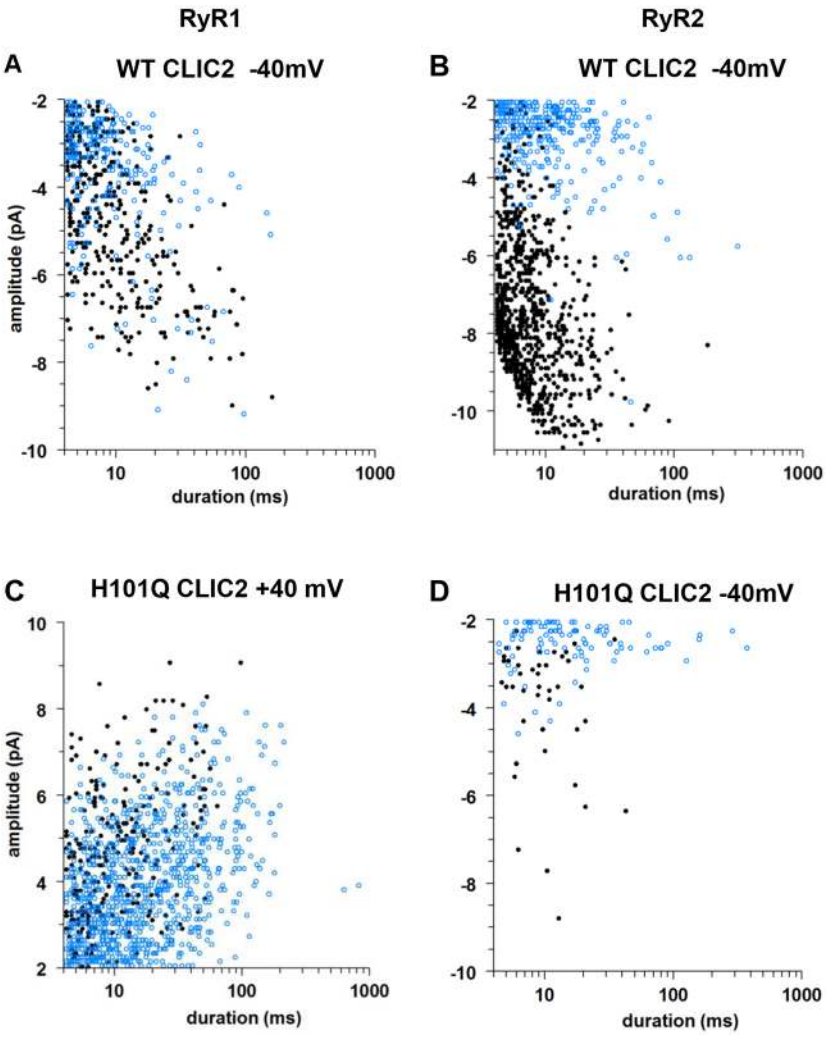

Fig. 2. Visualization of sub-state activity in open events with durations outside filter limitation (>4.5 ms). (A-D) The amplitude of every open event in ∼150 s of channel activity, filtered at 200 Hz, plotted as a function of its duration. The filled black circles show every event in the control current recorded before application of the CLIC2 construct. The blue circles represent every event in the currents recorded from the same channel after application of the CLIC2 construct. (A) A RyR1 channel with a control P_o of 0.08 at −40 mV, inhibited by WT CLIC2 (P_o=0.07). (B) A RyR2 channel at −40 mV (control P_o=0.06) inhibited by WT CLIC2 (P_o=0.04). (C) A RyR1 channel at +40 mV (control P_o=0.08) activated by H101Q (P_o=0.53). (D) A low-activity RyR2 channel at −40 mV (control P_o=0.006) activated by H101Q CLIC2 (P_o=0.04).

Journal of Cell Science (2017) 130, 3588-3600 doi:10.1242/jcs.204461

control with WT CLIC2 and most of the remaining openings were to sub-maximal levels, with open durations similar to those in control activity (Fig. 2A,B). With H101Q CLIC2, the number of openings increased and the duration of some low-amplitude events extended to >500 ms, in contrast to the control, where the longest sub-state events were ≤100 ms (Fig. 2C,D). There is a higher fraction of sub-state openings in the control RyR1 than in the control RyR2 channel activity (more black dots of <8 pA in Fig. 2A,C compared with B,D). This difference is significant in the average data in Fig. 3A.

There was a significant increase in the average percentage of sub-state openings after adding WT or H101Q CLIC2 to RyR1 and RyR2 channels and a trend towards a greater increase after exposure to H101Q CLIC2 compared with WT CLIC2, but the difference was not significant (Fig. 3A,B). The relative increase in sub-state activity was significantly greater in RyR1 than RyR2 with WT CLIC2, but not significantly different with H101Q CLIC2 (Fig. 3C). The effect of WT and H101Q CLIC2 on the overall open probability of the RyR channels was not altered by exclusion of brief events (Fig. 3D,E).

WT and H101Q CLIC2 proteins dissociate FKBPs from RyR channels

The effects of WT and H101Q CLIC2 on FKBP association with RyR1 and RyR2 was determined by exposing SR vesicles either to buffer alone (control) or to buffer containing WT or H101Q CLIC2, for 90 min. The RyRs and their associated proteins were then isolated using co-immunoprecipitation (co-IP), resolved by SDS-PAGE, blotted and immuno-probed with antibodies against RyRs, CLIC2 and FKBPs (Fig. 4A,B). There was a small but significant decline in FKBP12 associated with RyR1 after incubation with the

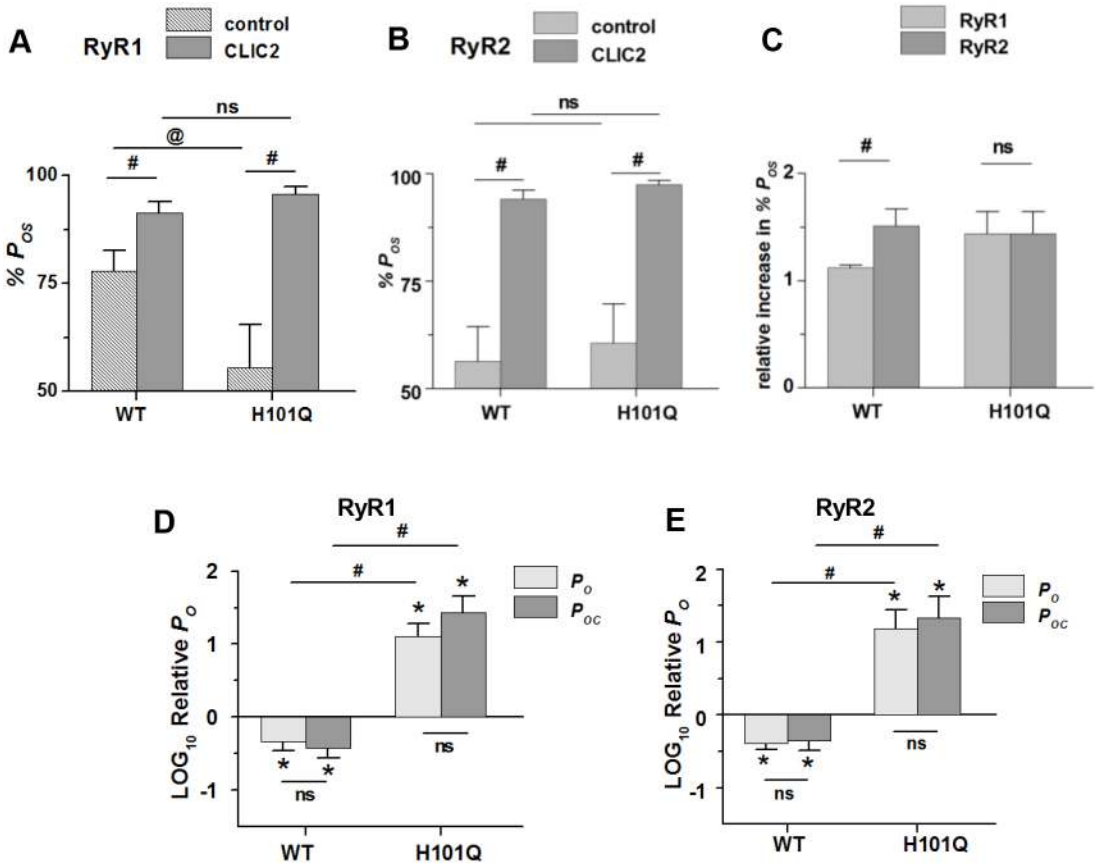

Fig. 3. The percentage of open probability attributable to sub-state activity (%P_{OS}) increases with both WT and H101Q CLIC2. (A) Average data for %P_{OS} before and after adding WT CLIC2 to RyR1 (n=3) or H101Q CLIC2 to RyR1 (n=10). Significance of differences between data in each graph was assessed by ANOVA with multidimensional Mahalanobis tests and P-values given for *post hoc* Fisher distances. In A, the increase in %P_{OS} is significant with WT CLIC2 added to RyR1 ($^{\#}P$=0.043) and H101Q CLIC2 to RyR1 ($^{\#}P$=0.0001), but there was no significant difference between %P_{OS} with WT or H101Q CLIC2 (ns), despite the decrease in P_o of all openings with WT CLIC2 and increase with H101Q CLIC2 as in D and E. There is an unusual significant difference ($^{@}P$=0.004) between mean control data for WT and H101Q CLIC2 because of the well-recognised variability between control P_o in RyR channels (Copello et al., 1997). (B) Average data for %P_{OS} before and after adding WT CLIC2 to RyR2 (n=6) or H101Q CLIC2 to RyR2 (n=8). The increase in %P_{OS} is significant with WT CLIC2 added to RyR2 ($^{\#}P$=0.001) or H101Q CLIC2 to RyR2 ($^{\#}P$<0.0001). As with RyR1 (A), there is no significant difference between %P_{OS} with WT or H101Q CLIC2 (ns; P=0.705), despite the number of openings declining with WT CLIC2 and increasing with H101Q CLIC2. (C) A comparison of the average relative increase in %P_{OS} in RyR1 and RyR2 after addition of WT or H101Q CLIC2. The increase in %P_{OS} with WT CLIC2 in RyR2 is significantly greater than in RyR1 ($^{\#}P$=0.042), but there was no significant difference in increases in %P_{OS} with H101Q CLIC2 between RyR1 and RyR2 (ns). (D,E) Average data for $\log_{10}$ relative P_o measured for all channel openings is compared with the relative $\log_{10}$ P_{oC} (P_o corrected for removal of filter limited events of <4.5 ms). The graphs show that removing filter-limited events has the same effect on control P_o and CLIC2-modified P_o, i.e. removing filter-limited events does not change the relative effects of WT and H101Q CLIC2 on RyR1 (D) or RyR2 (E). There is a highly significant difference between WT and H101Q CLIC2 ($^{\#}P$<0.0001) for both P_o and P_{oC} for RyR1 (D) and RyR2 (E) ($^{\#}P$<0.0001 in all cases), but no significant difference was seen between P_o and P_{oC} under any condition (ns). The asterisks in D and E indicate significant changes in P_o or P_{oC} after addition of WT CLIC2 to RyR1 (P=0.047 or 0.019, respectively) or RyR2 (P=0.013 or 0.004, respectively) and H101Q CLIC2 to RyR1 (P=0.0016 or 0.0003, respectively) or RyR2 (P=0.00129 or 0.00041, respectively). All data are presented as mean ±s.e.m.

Journal of Cell Science (2017) 130, 3588-3600 doi:10.1242/jcs.204461

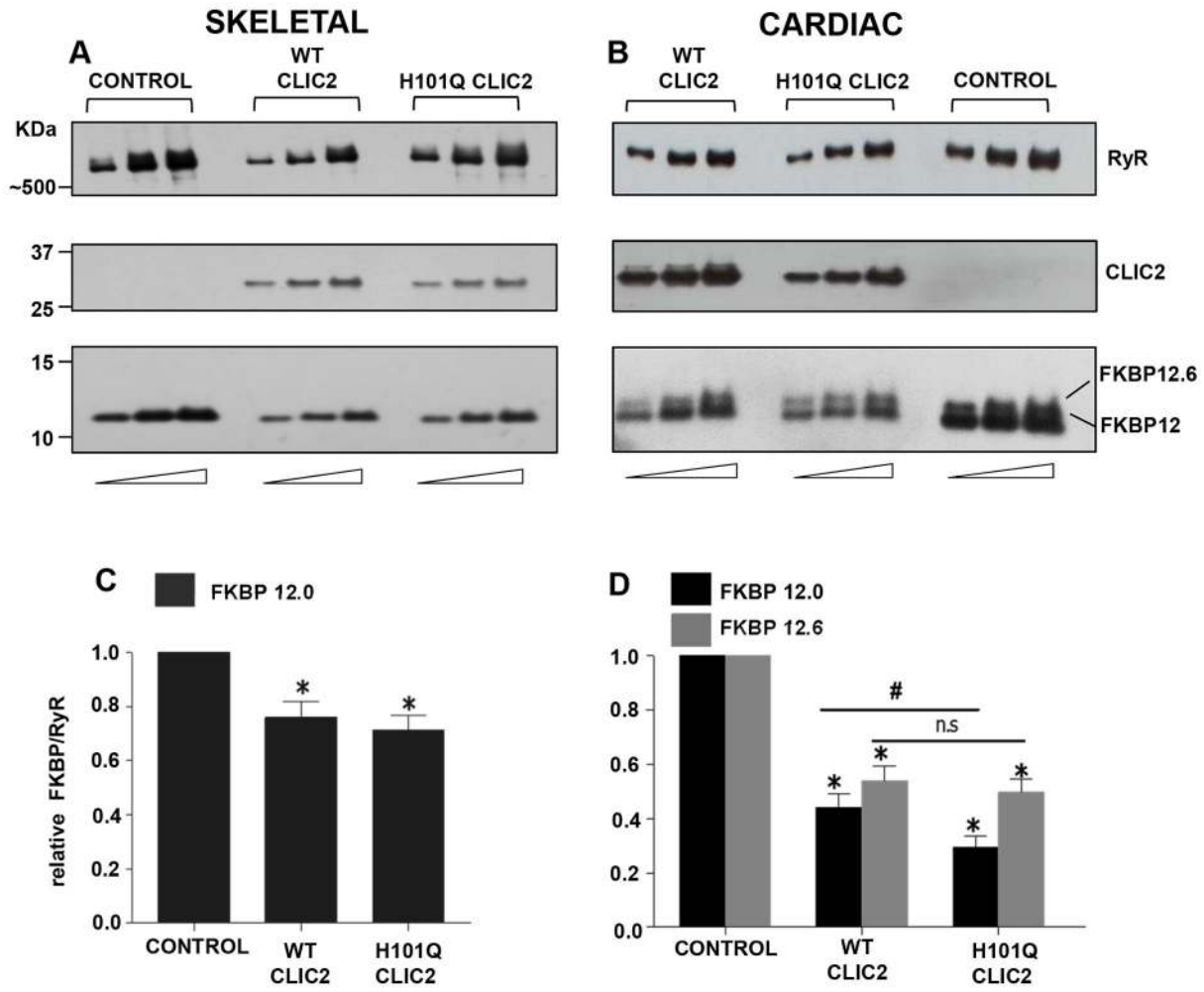

Fig. 4. Co-immunoprecipitation of RyRs with FKBP12 and FKBP12.6 bound in the absence and presence of WT or H101Q CLIC2. (A,B) Western blots of FKBP12 and/or FKBP12.6 associated with RyRs following incubation with CLIC2 constructs. In A, ~100 µg of skeletal SR vesicles was incubated with 8 µM WT CLIC2, 8 µM H101Q CLIC2 or with sample buffer (control) as indicated, followed by RyR co-IP. In B, ~100 µg of cardiac SR vesicles was incubated with 8 µM WT CLIC2, 8 µM H101Q CLIC2 or with sample buffer (control) as indicated, followed by RyR co-IP. In A and B, 5, 10, or 15 µl of each co-IP sample (increasing amounts indicated under the lanes) were run on SDS-PAGE, transferred to PVDF membrane and probed for RyR, CLIC2 and FKBP. (C,D) Average densitometry ratios for FKBP12/RyR1 (C) or FKBP12/RyR2 and FKBP12.6/RyR2 (D). WT or H101Q CLIC2 densitometry measurement is expressed relative to control densitometry measurement. Data are presented as mean±s.e.m. (N=12 for RyR2 and N=9 for RyR1), the asterisks indicate a significant difference from control and the hash (#) indicates a significant difference between WT and H101Q CLIC2; n.s, no significant difference between the effects of WT CLIC2 and H101Q CLIC2 treatments. Significance was determined using ANOVA and *post hoc* Fisher distances, P<0.05.

CLIC2 proteins, but no significant difference between WT and H101Q CLIC2 (Fig. 4A,C). Amounts of FKBP12 and FKBP12.6 associated with RyR2 were significantly reduced after incubation with WT CLIC2 (Fig. 4B, left lanes), compared with amounts in the control lane following incubation with buffer alone (Fig. 4B, right lanes). There was a greater reduction in FKBP12, but not FKBP12.6, after incubation with H101Q CLIC2 (Fig. 4B, middle lanes). These changes are reflected in the average data in Fig. 4D. Immuno-probing with the anti-CLIC2 antibody confirmed that WT and H101Q CLIC2 were bound to both RyR1 and RyR2 (Fig. 4A,B).

Is sub-state activity in the presence of CLIC2 related to FKBP dissociation from RyRs

The percentage of sub-state opening (%P_{oS}) is plotted against relative FKBP binding in Fig. 5A-C. It is clear that the percentage of sub-state opening increases as FKBP binding declines in all cases, and that this relationship is apparently stronger for FKBP12 and FKBP12.6 with RyR2 (Fig. 5B,C) than in FKBP12 with RyR1 (Fig. 5A). The weaker relationship with RyR1 was due to the combined effects of a smaller reduction in FKBP12 following CLIC2 binding and a greater percentage of sub-state activity in the control RyR1 activity before addition of WT or H101Q CLIC2. In contrast to the consistent relationship between the relative amounts of sub-state activity and FKBP binding (Fig. 5A-C), the relationship between the overall open probability of the channels (P_o) and FKBP binding was variable (Fig. 5D-F). A positive slope between P_o and FKBP binding with WT CLIC2, in contrast to the negative slope with H101Q CLIC2. The effects of WT and H101Q CLIC2 on absolute P_o were significant according to the sign test, as P_o fell in all channels exposed to WT CLIC2 and increased in all channels exposed to H101Q CLIC2.

CLIC2 proteins do not bind to FKBP12 and FKBP12.6

The mechanisms underlying the ability of the CLIC2 proteins to dissociate FKBPs from the RyRs may have depended on CLIC2

Journal of Cell Science (2017) 130, 3588-3600 doi:10.1242/jcs.204461

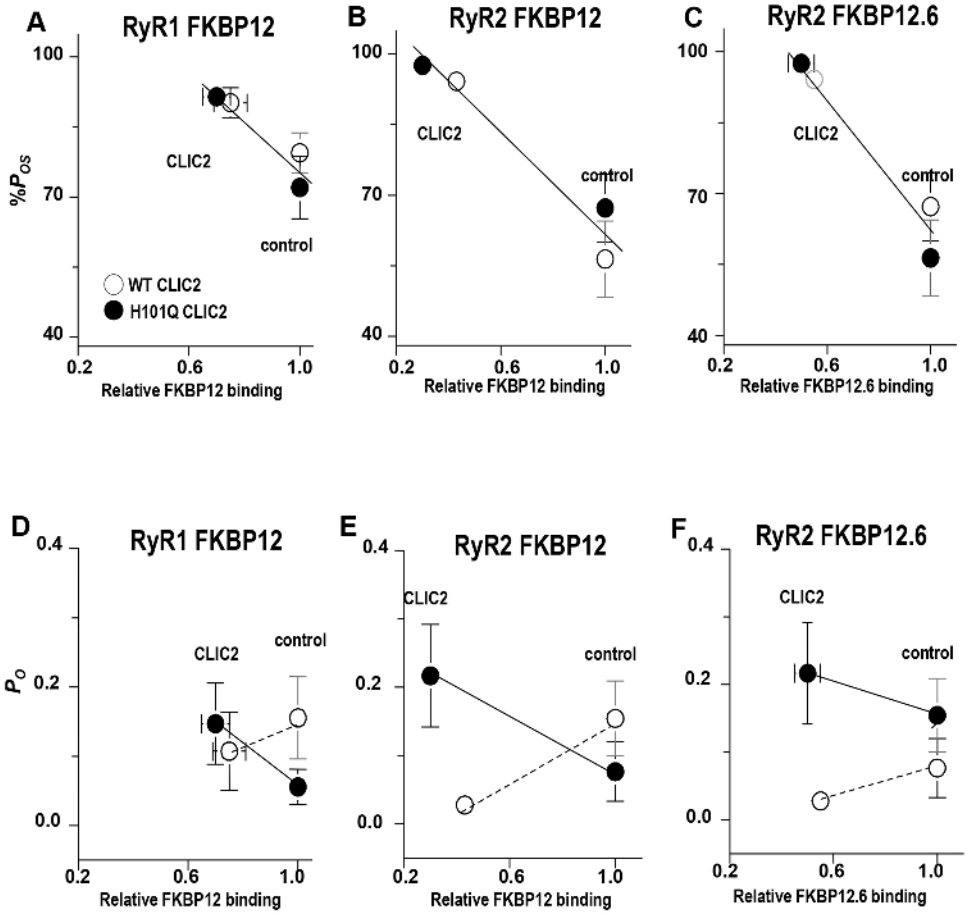

Fig. 5. Relationship between channel activity and FKBP binding to RyRs. (A-C) Average data for $\%P_{OS}$ plotted against the average relative densitometry data for FKBP12/RyR1 (A), FKBP12/RyR2 (B) and FKBP12.6/RyR2 (C). (D-F) Average data for the probability values for all open events longer than 4.5 ms (P_{OC}) plotted against the average relative densitometry data for FKBP12/RyR1 (D), FKBP12/RyR2 (E) and FKBP12.6/RyR2 (F). In A-F, the open circles indicate average data for WT CLIC2 and the filled circles indicate average data for H101Q CLIC2. The vertical error bars show the s.e.m. for average $\%P_{OS}$ or P_{OC} data and the horizontal error bars show s.e.m. for average relative FKBP/RyR data. Error bars not visible are contained within the dimensions of the symbols.

binding either to the RyRs or to the FKBPs, or indeed, binding to both proteins. Since CLIC2 does bind to RyR1 and causes a substantial conformational change in a region that impinges on the FKBP binding site (Meng et al., 2009), its binding to the RyRs could disrupt FKBP binding. Since FKBP binding to RyRs is disrupted when rapamycin or FK506 bind to FKBPs, it is likely that CLIC2 binding to FKBPs might contribute to FKBP dissociation. Cross-linking methods were first used to determine whether CLIC2 does bind to FKBP12 (Fig. 6). An interaction between the proteins would result in a CLIC2–FKBP conjugate that would appear within the red box drawn over the final column in each blot in Fig. 6, at ~37 kDa. No protein was detected in this region by antibodies against either CLIC2 (Fig. 6A) or FKBP (Fig. 6B).

The absence of direct binding of FKBP12 to CLIC2 was confirmed with microscale thermophoresis (MST) using fluorescently labelled CLIC2. In order to validate the technique for detecting binding events with CLIC2, a control experiment was performed where an anti-CLIC2 antibody was titrated against 720 nM CLIC2 protein. Fig. 6C shows that as expected, a binding event of <100 nM was observed between CLIC2 and its antibody. In contrast, titration of FKBP at concentrations ranging from 13 nM to 10 µM (Fig. 6D) against 5.72 µM CLIC2 (within the range of CLIC2 concentrations used to dissociate FKBP and used to influence RyR activity) resulted in a scattered profile suggesting that there was no binding. This experiment was repeated using three different concentrations (720 nM, 5.72 µM and 8.72 µM) of CLIC2 protein, with no evidence of direct binding at any concentration (Fig. S2). Therefore, we conclude that, in contrast to rapamycin and FK506, CLIC2-induced dissociation of FKBPs was due mainly to CLIC2 binding to RyRs and changing the conformation of the FKBP binding site and its affinity for the FKBPs.

Comparison of effects of CLIC2, rapamycin and FK506 on FKBP binding to RyR1 and RyR2

Two points arise from the study of FKBP–RyR dissociation following exposure to CLIC2. Firstly, the efficacy of CLIC2 in dissociating FKBP was less with RyR1 than with RyR2 (Fig. 4 above) and secondly, the dissociation was not caused by CLIC2 binding to FKBPs (Fig. 6), unlike dissociation with rapamycin or FK506, which bind to the FKBPs. Therefore, it was of interest to compare the efficacy of CLIC2, rapamycin and FK506 in dissociating the FKBPs from RyR1 and RyR2. Cardiac and skeletal SR vesicles were incubated with rapamycin for 90 min, then subjected to RyR co-IP (Fig. 7A-D). The results were in marked contrast to the limited dissociation of FKBP12 from RyR1 caused by CLIC2 (Fig. 4). Rapamycin and FK506 binding to FKBP12 were equally efficient in removing substantial (~90-98%) FKBP12 from RyR1 (Fig. 7A,C,E). Again, in contrast to CLIC2, neither FK506 nor rapamycin removed FKBP12 from RyR2 and, while there was significant dissociation of ~70-80% of the FKBP12.6 from RyR2 with rapamycin, there was effectively no dissociation of FKBP12 (Fig. 7B,D,F,G). Therefore, CLIC2 was far more effective than rapamycin or FK506 in removing FKBP12 from RyR2, whereas rapamycin and CLIC2 were similarly effective in dissociating FKBP12.6. Although FKBP12.6 has a higher affinity for RyR2 than FKBP12 (Guo et al., 2010; Jeyakumar et al., 2001;

Journal of Cell Science (2017) 130, 3588-3600 doi:10.1242/jcs.204461

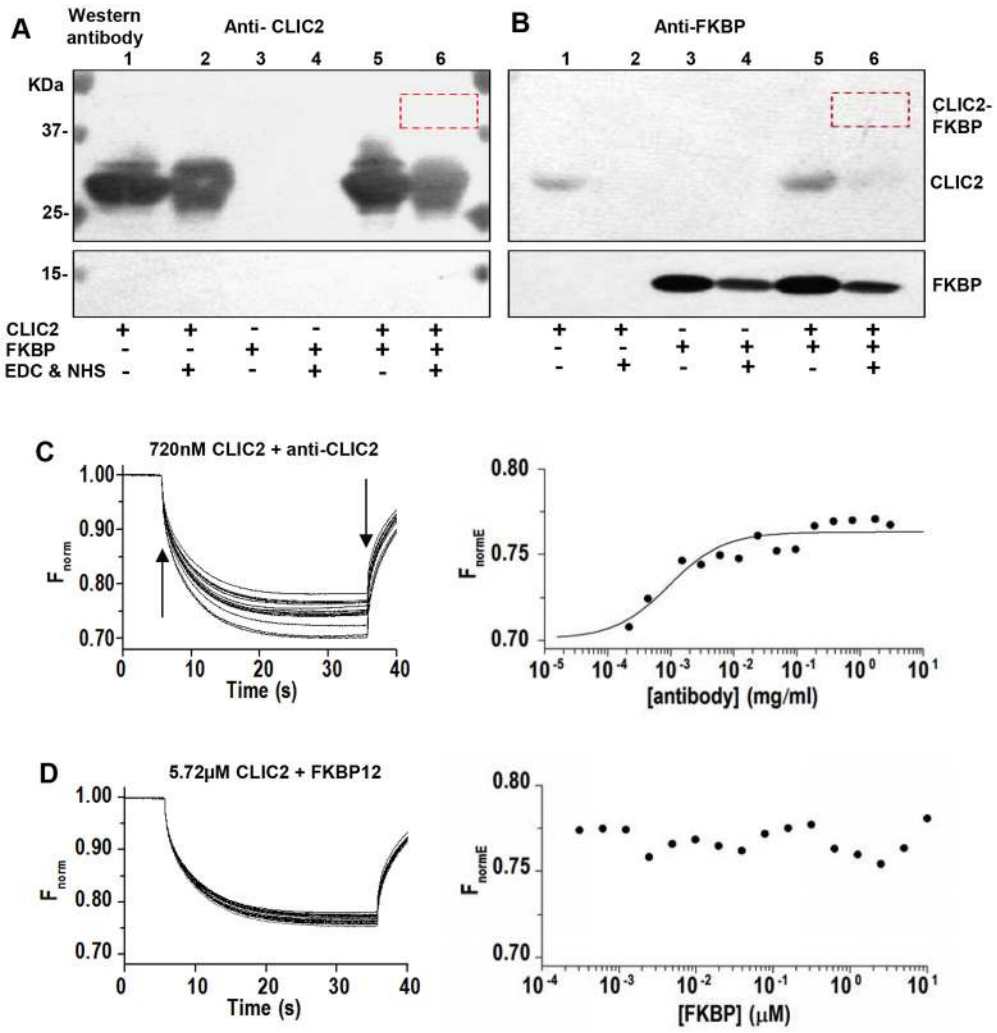

Fig. 6. FKBP does not bind significantly to CLIC2. (A,B) Zero length cross-linking. FKBP isolated from cardiac SR vesicles and recombinant H101Q CLIC2 was incubated alone or with cross-linking agents EDC and NHS. The proteins were separated by SDS-PAGE and immuno-probed on Western blots with anti-CLIC2 antibody and anti-FKBP antibody. The experiment was performed under six conditions: (1) CLIC2 only, (2) CLIC2+cross-linkers, (3) FKBP only, (4) FKBP+cross-linkers, (5) CLIC-2+FKBP, and (6) CLIC-2+FKBP+cross-linkers. Inclusion in the incubation sample added to each lane is indicated by (+), and exclusion is indicated by (–) beneath each lane. Only the far right lane in each blot contained FKBP12, CLIC2 and cross-linkers. If present, a CLIC2–FKBP conjugate would be detected in these lanes at ~37 kDa (red box) by both anti-CLIC2 and anti-FKBP in the region. The blot was probed with anti-CLIC2 (A) and with anti-FKBP (B). (C,D) Microscale thermophoresis. The normalised fluorescence signal (F_{norm}) is shown as a function of time during thermophoresis in the left-hand graph in each pair. The laser, initiating the temperature jump and thermophoresis, was switched ON at the time indicated by the first arrow in C and switched OFF at the time indicated by the second arrow in C. The right-hand graph in each pair shows the normalised fluorescence measured immediately before the end of the thermophoresis (F_{normE}) plotted as a function of potential binding partner concentration. Filled symbols show normalised fluorescent measurements for each binding partner concentration. The binding partner concentrations are serial dilutions of 6.3 mg/ml of anti-CLIC2 antibody added to 720 nM CLIC2 (C) or serial dilutions of 10 μM FKBP12 added to 5.72 μM CLIC2 (D). The fluorescence signal in C shows a clear increase in F_{normE} with increasing antibody concentration, indicative of an interaction. The curve through the data in C is a binding curve generated by standard Monolith NT.115, NanoTemper software. The final normalised fluorescence in D is independent of FKBP concentration, indicating that there is no interaction between CLIC2 and FKBP12.

Timerman et al., 1993), FKBP12 was more resistant to removal from RyR2 than FKBP12.6 using the two compounds that bind to FKBP12 and FKBP12.6 under our conditions.

DISCUSSION

In summary, we show a strong relationship between the percentage of RyR channel openings to sub-state levels and the amount of associated FKBP12 and FKBP12.6 in native channels, both prior to and after, exposure to WT and H101Q CLIC2. This is the first report of increased sub-state activity correlated with dissociation of FKBP12 and FKBP12.6 following the binding of an endogenous ligand to RyR channels. The results suggest that conformational changes resulting from CLIC2 binding to the RyRs can allosterically alter the FKBP binding site, probably reducing its affinity for the FKBPs and releasing these immunophilins from the channel protein complex. In addition, we show distinct FKBP and RyR isoform-specific differences between the abilities of CLIC2, rapamycin and FK506 to dissociate FKBP12 and FKBP12.6 from RyR2 or FKBP12 from RyR1.

FKBP12 and FKBP12.6 are bound to sheep cardiac RyR2

There is a strong species dependence in the expression of FKBP12 and FKBP12.6 in heart. Relative amounts of FKBP12 in heart are: 0 pmol/mg SR in rat; 0.58 pmol/mg SR in rabbit; 1.74 pmol/mg SR in pig; 48.6 pmol/mg SR in mouse, compared with 38 pmol/mg skeletal SR in rabbit. FKBP12.6 in skeletal

Journal of Cell Science (2017) 130, 3588-3600 doi:10.1242/jcs.204461

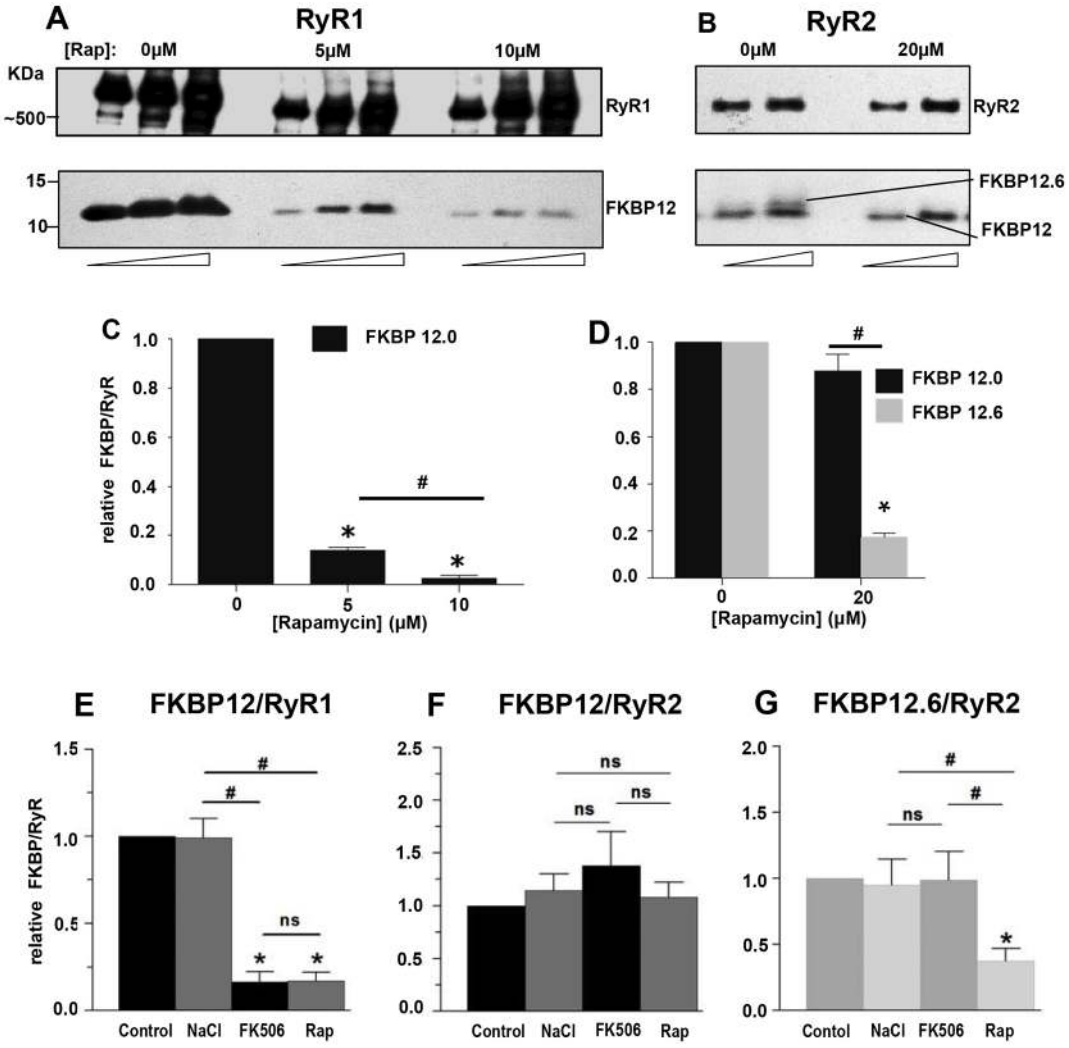

Fig. 7. Efficacy of rapamycin, FK506 and 600 mM NaCl in dissociating FKBP12 and 12.6 from RyRs. (A,B) Western blots of FKBP12 and/or FKBP12.6 associated with RyRs following incubation with rapamycin. (A) Approximately 100 µg of skeletal SR vesicles was incubated with buffer or buffer plus 5 or 10 µM rapamycin as indicated, for 90 min at RT, followed by RyR co-IP; then, 5, 10, or 15 µl of each co-IP sample were run on SDS-PAGE (increasing amounts indicated under the lanes). (B) Approximately 100 µg of cardiac SR vesicles were incubated with buffer or buffer plus 20 µM rapamycin as indicated, for 90 min at RT, followed by RyR co-IP; then, 10 or 15 µl of each co-IP sample were run on SDS-PAGE (increasing amounts indicated by arrows under the lanes). In A and B, co-IP samples were eluted with 40 µl of 2× SDS-PAGE buffer after washing and 20 µl of each sample run on SDS-PAGE, then transferred to PVDF membrane and probed for RyR and FKBP. (C,D) Average densitometry ratios (±s.e.m.) for FKBP12/RyR1 (n=12) (C) or FKBP12/RyR2 and FKBP12.6/RyR2 (n=12) (D). Treatment densitometry ratios are expressed relative to control densitometry ratios. The asterisks indicate a significant difference from control. The hash (#) indicates a significant difference between 5 µM and 10 µM rapamycin treatment of RyR1 in C or between FKBP12 and FKBP12.6 association with RyR2 in D. Significance was determined by ANOVA and *post hoc* Fisher analysis, P<0.05. (E-G) Mean densitometry data from western blots, expressed in the same way as in C and D, comparing the effects of incubation of ~150-200 µg of RyR1 SR vesicle protein (n=14) and ~100-150 µg of RyR2 SR vesicle protein (n=7) with buffer (control), 10 µM rapamycin, 10 µM FK506 or 600 mM NaCl for 90 min at 37°C, followed by RyR co-sedimentation analysis of FKBP12 associated with RyR1 (E) FKBP12 associated with RyR2 (F) and FKBP12.6 associated with RyR2 (G). Data presented as mean±s.e.m. The asterisks indicate a significant difference from control. The hash (#) indicates a significant difference between FKBP12 associated with RyR1 in E or between FKBP12 or FKBP12.6 association with RyR2 in E and F, respectively. Significance in E and F was determined by ANOVA with multidimensional Mahalanobis analysis and P-values given for *post hoc* Fisher distances with P<0.05; ns indicates no significant difference.

muscle varies from: 0 pmol/mg SR in rabbit; 0.3 pmol/mg SR in pig; 0.48 pmol/mg SR in mouse; to 0.63 pmol/mg SR in rat (Zissimopoulos and Lai, 2009). Thus, there is a FKBP12: FKBP12.6 ratio of 100:1 for mouse RyR2, but 0:1 for rat RyR2. Immunoblotting of rat myocyte homogenate (in contrast to isolated SR) showed a FKBP12:FKBP12.6 ratio of ~10:1 (Guo et al., 2010), suggesting significant loss of FKBP12 from rat SR during microsomal preparation. Our results suggest that sheep are similar to mice in that both FKBP12 and FKBP12.6 are clearly associated with RyR2.

Sub-state activity and FKBP binding to RyRs

While it is generally accepted that removal of FKBP12 from RyR1 leads to an increase in RyR1 activity and channel opening to sub-state levels, it is not clear whether this is also the case with RyR2. Sub-state activity is observed in RyR2 from FKBP12 knockout mice (Shou et al., 1998) and increased sub-state activity is reported after removal of FKBP12.6 from RyR2 (Marx et al., 2000; Wehrens et al., 2003), although others find that neither FKBP12.6 nor FKBP12 influences sub-state activity (Xiao et al., 2007; Galfré et al., 2012). Part of the difference probably depends on a lack of

Journal of Cell Science (2017) 130, 3588-3600 doi:10.1242/jcs.204461

quantification or definition of a sub-state opening. Here, we define a sub-state event as an opening of any duration outside filter limitations, to any level above the baseline noise and less than the maximum conductance. The percentage of open probability attributable to such sub-state events is correlated with amounts of FKBP bound to RyR1 and RyR2 in the absence (control) and presence of WT and H101Q CLIC2. The significant sub-state opening in control activity particularly in RyR1 implies that, if sub-state opening is related to FKBP binding, then RyRs in SR vesicles are not fully saturated with FKBPs.

There is a significant fraction of channel opening to low conductance sub-state levels in hyperactive RyR channels exposed to H101Q CLIC2, which would contribute substantially to current flow from the SR and increases cytoplasmic Ca^{2+} levels. Such openings would also contribute to hyperactivity induced by mutations or acquired modifications that lead to arrhythmia, skeletal myopathies or neuropathies. Therefore, measurements of the effects of mutations or acquired modification on channel activity should include low-conductance openings to discern the full impact of the mutation or modification on Ca^{2+} release from intracellular stores. In contrast to activating mutations and H101Q CLIC2, WT CLIC2 substantially reduces the open probability of RyR channels, and indeed, it appears that some of the full openings are replaced by low-conductance openings in the presence of the WT protein. Therefore, the conversion of full openings to sub-state opening further reduces the total current (leak) though RyR channels. Thus, although WT and H101Q CLIC2 have similar effects on the proportion of channel openings to sub-state levels, the effect on 'leak' through the RyRs is vastly different and dictated by the overall inhibitory action of WT CLIC2, in contrast to the overall excitatory action of H101Q CLIC2.

Resistance of FKBP12 and FKBP12.6 to dissociation from RyR2 by rapamycin or FK506

Our data showing that rapamycin and FK506 did not dissociate FKBP12 from RyR2 and that rapamycin alone dissociated some FKBP12.6 are consistent with previous data (Zissimopoulos and Lai, 2009; Guo et al., 2010). In addition, cyclic ADP-ribose (cADPR), is a physiological ligand that binds to FKBP12.6 (Noguchi et al., 1997; Zhang et al., 2009), but like rapamycin and FK506, is inefficient in removing the FKBPs from RyR2 (Zissimopoulos and Lai, 2009). The resistance of RyR2-bound FKBP12 and 12.6 to dissociation by compounds that bind to FKBPs could be due to the compound's binding site on the FKBPs being occluded when the FKBPs are bound to RyR2. An alternative possibility is that the compounds bind to the FKBPs, but the effects of their binding are not sufficient to displace the FKBPs from RyR2. Notably, as these compounds bind to FKBP12 and dissociate it from RyR1 (Zissimopoulos and Lai, 2009), either the binding sites for the compound are not occluded in RyR1 or the effects of compound binding are sufficient to displace FKBP12. This then suggests that the affinity of RyR2 for FKBP12 and FKBP12.6 is higher than that of RyR1 for FKBP12. By contrast, when CLIC2 binds to the RyRs, its impact on the FKBP binding site is greater in RyR2 than in RyR1.

FKBP binding to RyRs can depend on RyR open probability

Unlike the inconsistent relationship between overall P_o and FKBP binding to RyRs in the presence of CLIC2 proteins (Fig. 5D-F), FKBP binding to RyRs under other conditions can be modified by the activity of the ion channel. RyR1 activating factors (1 µM free Ca^{2+}, 1 µM free Ca^{2+} plus 1 mM ATP or 10 mM caffeine) reduce amounts of FKBP12 bound to RyR1, whereas inhibitory factors (1 mM EGTA, 1 mM free Ca^{2+}, 1 µM ruthenium red) increase FKBP12 binding (Jones et al., 2005). Similarly, FKBP12 binding to RyR1 is reduced in skeletal muscle weakness with increased RyR1 activity and Ca^{2+} leak from SR (Reiken et al., 2003). Leaky RyR1 channels from dystrophic or malignant hyperthermic (MH) mouse muscle are *S*-oxidized (Mei et al., 2013) and *S*-nitrosylated (Durham et al., 2008; Bellinger et al., 2009), and both modifications can lead to FKBP12 depletion (Zissimopoulos et al., 2007; Aracena et al., 2005). Central core disease (CCD) mutations causing leaky RyR1 impinge on the FKBP binding site (Zhu et al., 2013; Yan et al., 2015). In the heart, RyR2 is hyperactive and leaky in heart failure, stress or with mutations that underlie arrhythmia that is often fatal. There are numerous reports that the RyR2 channels in these conditions have less than the normal complement of associated FKBP12.6 (Wehrens et al., 2005). Together, these results indicate a general negative correlation between overall P_o and FKBP binding. That CLIC2 does not fit with this general trend is consistent with other unusual effects of CLIC2 on RyR channels (Jalilian et al., 2008; Meng et al., 2009).

Paradoxical effects of CLIC2 on RyR channels

WT CLIC2 binds across the domain 5–6 interface in the RyR1 clamp region and, at the same time separates domains 9 and 10 as also seen in the channel 'open' configuration (Meng et al., 2009). An increase in [^{3}H]ryanodine binding in the presence of CLIC2 is consistent with the 'open' structure of domains 9 and 10 (Meng et al., 2009). By contrast, P_o falls in the presence of WT CLIC2 (Fig. 1 and Dulhunty et al., 2005; Meng et al., 2009). These paradoxical effects are explained if the 'open' conformational change allows increased [^{3}H]ryanodine binding, whereas CLIC2 binding to domains 5–6 stabilizes the channel closed state (Meng et al., 2009). The fact that FKBP12 and FKBP12.6 are dissociated by exposure to WT and H101Q CLIC2 is consistent with this explanation if H101Q CLIC2 binding also separates domains 9 and 10. This conformational change could impact the FKBP binding site that lies under (with respect to the t-tubule surface of RyR1) domains 9–10 within an angle formed with domain 3 (Samsó et al., 2006). Since H101Q CLIC2 activates channels, H101Q CLIC2 may alter the domain 5–6 interaction and channel closure. There appears to be a fine line between CLIC2 stabilizing or destabilizing the channel, as WT CLIC2 can increase the probability of the channel being open if the redox potential is reducing (Jalilian et al., 2008). Thus, small conformational changes in CLIC2 or its binding site may interconvert domain 5–6 instability to stability and hence pore closing and opening.

Effects of the H101Q CLIC2 mutation on skeletal muscle function

Changes in skeletal muscle function were not specifically reported with the H101Q mutation (Takano et al., 2012) as there was no record of skeletal muscle function. It is likely that skeletal muscle function was not examined because the overwhelming impact of the cardiac and intellectual phenotype masked any less-severe skeletal muscle phenotype. It is also possible that any skeletal muscle phenotype was weaker than the cardiac effects because of a weaker effect of CLIC2 on FKBP12 association with RyR1 than with RyR2. There may well have been skeletal muscle weakness and histological changes indicative of excess Ca^{2+} leak from RyR1 if appropriate testing had been performed. The results of the present study suggest that skeletal muscle function should be examined in the future in patients with CLIC2 mutations and will be relevant to skeletal muscle weakness that might be detected.

Journal of Cell Science (2017) 130, 3588-3600 doi:10.1242/jcs.204461

The pH dependence of CLIC2 activity

It is established that there is a CLIC2 metamorphosis when pH is lowered from pH 7.3 to values between pH 6.0 and pH 5.0. The protein changes from a soluble form in the cytoplasm to a lipid-penetrating form and inserts into the membrane to form a Cl^- channel from which its name is derived (Cromer et al., 2007). Similar WT and H101Q CLIC channel activity has been observed in bilayers at pH 5 where Cl^- is the major current carrier (Takano et al., 2012). This activity is not observed in bilayers at pH7.4 with $CsCH_3O_3S^-$ as the major anionic current carrier, i.e. conditions used to observe RyR channel activity (Takano et al., 2012; Board et al., 2004). Curiously, the summed activity of multiple CLIC2 channels at pH5, in Cl^--containing solutions, appears similar to non-specific currents seen during bilayer breakdown, and indeed can eventually lead to bilayer breakdown (Takano et al., 2012). Such activity may have been attributed to bilayer breakdown in our early studies (Takano et al., 2012; Board et al., 2004). We were unable to study the effects of low pH on the action of CLIC2 on RyR channel activity because RyR activity is effectively abolished at pH less than 6.8 (Laver et al., 2000). The effect of pH on the ability of CLIC2 to dissociate FKBPs from RyRs is of interest, but was not within the scope of the present experiments in which the focus was on interactions that impact RyR function in the living cell. Cytoplasmic pH is tightly controlled in muscle to pH 7.0-7.4, although it can fall to levels around pH 6.8 after extreme exercise in skeletal muscle (Laver et al., 2000), it is unlikely that such levels are achieved in the vicinity of the RyR as pH-induced abolition of RyR activity would cause muscle paralysis.

Conclusions

We have measured sub-state opening using a novel analysis protocol, and show a novel and strong relationship between sub-state gating and FKBP binding following incubation with WT CLIC2 or its H101Q mutant. The increase in sub-state activity was independent of whether the channels were inhibited by WT CLIC2 or activated by H101Q CLIC2, but the long-lived sub-state openings in the presence of H101Q CLIC2 would contribute to a leaky channel phenotype and to the intellectual and cardiac problems associated with the H101Q mutation. The results strongly support the notion that the opening of RyR channels to sub-state levels is determined by the amounts of FKBP12 and/or FKBP12.6 bound to the channels. The results provide unprecedented insight into factors impacting FKBP binding to RyR channels and regulating its activity in health and disease.

MATERIALS AND METHODS

Mutagenesis, expression and purification of CLIC2

H101Q CLIC2 mutagenesis was performed as previously described (Takano et al., 2012). Recombinant WT and H101Q CLIC2 were expressed in *E.coli* from a pHUE vector with an N-terminal poly-His tag and purified by Ni-agarose affinity chromatography (Board et al., 2004; Dulhunty et al., 2005). The concentrations of purified CLIC2 and H101Q CLIC2 protein were adjusted to 6 mg/ml in HEPES buffer (50 mM HEPES, pH7.4, 200 mM KCl and 10% glycerol). The CLIC2 protein samples were divided into single-use aliquots and stored at –70°C.

GST–FKBP12 expression and purification

GST–FKBP12 in a pGEX2TK vector was expressed in *E.coli* and purified by glutathione-agarose affinity chromatography (Mackrill et al., 2001). GST–FKBP12 protein was adjusted to 1.1 mg/ml and exchanged into MOPS buffer (20 mM MOPS, 150 mM NaCl, pH 7.4).

SR vesicle isolation

Cardiac SR vesicles were prepared from sheep heart (Australian National University Farm; Dulhunty et al., 2005). Ventricles were diced and homogenised in cardiac homogenising buffer (CHB; 290 mM sucrose, 10 mM imidazole, 0.05 mM DTT and 3 mM NaN_3, pH 6.9), centrifuged at 11,000 ***g*** for 20 min at 4°C, the supernatant filtered through cotton gauze, then centrifuged at 110,000 ***g*** for 2 h at 4°C. The pellet was resuspended in CHB plus 649 mM KCl, incubated on ice for 30 min and centrifuged at 7000 ***g*** for 10 min at 4°C. The supernatant was centrifuged at 180,000 ***g***, the P4 pellet resuspended and homogenised in 15 ml CHB plus 649 mM KCl and stored at −70°C.

Back and leg muscle dissected from New Zealand white rabbits (Research School of Biological Sciences, Australian National University; Saito et al., 1984; Ahern et al., 1994, 1997) was rinsed and diced in phosphate buffered saline (PBS): 137 mM NaCl, 7 mM Na_2HPO_4, 2.5 mM $NaH_2PO_4{\bullet}H_2O$, 2 mM EGTA (ethylene glycol-bis[b-aminoethyl ether]N,N,N',N'-tetraacetic acid, pH 7.4) and stored at −70°C. Muscle was homogenized four times in skeletal homogenising buffer (SHB): 20 mM imidazole and 300 mM sucrose, pH 7.4, centrifuged at 11,000 ***g*** for 20 min at 4°C, the pellet suspended in SHB, homogenised and centrifuged at 11,000 ***g*** for 20 min at 4°C. The supernatant was filtered through cotton gauze, centrifuged at 110,000 ***g*** for 2 h at 4°C. The pellet was resuspended and re-homogenised in SHB, centrifuged in a discontinuous sucrose gradient at 70,000 ***g*** for 16 h at 4°C. B3 and B4 fractions were collected, diluted in 20 mM imidazole, centrifuged at 125,000 ***g*** for 1 h at 4°C, the pellet resuspended in SHB buffer and stored at −70°C. Protein concentrations, determined using DC Protein Assay kits, were 10-15 mg/ml in cardiac P4 and 15-20 mg/ml skeletal B3.

Isolation of FKBP12.0 and FKBP12.6 from microsomal SR vesicle preparations

Preliminary experiments required the use of FKBP12.0 and FKBP12.6, which were initially obtained from SR vesicle preparations (Galfré et al., 2012). 300 µg of cardiac SR vesicle preparation was incubated for 5 min (4°C) in 50 µl of a buffer composed of 80 mM MOPS, 600 mM NaCl and 1 mM $CaCl_2$ (40 µM free Ca^{2+}, with BAPTA), pH 7.4. The sample was centrifuged at 13,000 rpm for 20 min; with the resulting pellet retaining the RyR, while the supernatant contained free proteins, including FKBP12.0 and FKBP12.6. The supernatant was centrifuged again (13,000 rpm for 20 min) to pellet remaining SR debris, the supernatant collected and diluted 4-fold with milliQ water to bring the [NaCl] to 150 mM. The solution contained proteins that were not bound to RyRs, including FKBP12.0 and FKBP12.6 (Fig. S3). As co-IP experiments (Fig. 7) show that 600 mM NaCl does not dissociate any more FKBP12 or FKBP12.6 from RyRs than incubation in buffer alone, either the isolated FKBPs were not initially bound to RyRs, or incubation alone is sufficient to dissociate the FKBPs.

Single-channel recording and analysis

As described previously (Beard et al., 2008; Wium et al., 2012), SR vesicles were incorporated into lipid bilayers in solutions containing *cis*: 230 mM $CsCH_3O_3S$, 20 mM CsCl, 1 mM $CaCl_2$ and 10 mM N-Tris[hydroxymethyl] methyl-2-aminoethanesulfonic acid (TES; pH 7.4); and *trans*: 30 mM Cs $CsCH_3O_3S$, 20 mM CsCl, 1 mM $CaCl_2$, and 10 mM TES (pH 7.4). Following SR vesicle incorporation, *cis* (cytoplasmic) Ca^{2+} was adjusted to 1 µM or 100 nM with BAPTA, determined using a Ca^{2+} electrode and *trans* [$CsCH_3O_3S$] was increased to 230 mM. *Trans* [Ca^{2+}] was 1 mM throughout. Open probability (P_o) was measured with the program Channel 2 (Michael Smith and Peter Gage, JCSMR, Canberra, Australia).

Sub-state analysis was performed on 100-150 s of recorded current, filtered with a 200 Hz Gaussian filter. A sub-state opening was defined as any channel opening that was longer than 4.5 ms (to exclude filter-limited events), with an open amplitude greater than the baseline noise [~10% of the maximum open level and less than ~90% of the maximum single channel conductance (G_{max})]. The 10% to 90% range was considered optimal given the noise level observed with the 200 Hz filter used to evaluate sub-state activity. Noise with the 200 Hz filter was ~0.5 to 0.8 pA, i.e. ~5-8% of G_{max} (~10 pA) in these experiments. Therefore the cut-off was set at 10% to avoid noise transients being falsely detected as channel openings. The ~0.5-0.8 pA noise similarly prevents openings between 90 and 100% G_{max} being confidently discriminated from G_{max}. It is likely that the 10-90% detection protocol excluded some small conductance openings and also some sub-state openings close to maximal opening. Confining substrate openings to levels within a narrower range (e.g. 20-80% G_{max}), would have excluded a larger number of openings to levels that are outside the baseline noise and less than maximal opening (see Fig. 2).

Journal of Cell Science (2017) 130, 3588-3600 doi:10.1242/jcs.204461

To determine the fraction of sub-state opening, the probability of all open events, P_o, was measured using a threshold discrimination set at ∼10% of the maximum conductance, then a corrected P_{oC} calculated for all events ≥4.5 ms. The probability of opening to the maximum conductance $P_{o\ max}$ was measured with the open threshold discriminator set at ∼90% of the maximum conductance. The percentage of channel openings to sub-state levels $\%P_{oS}$ was then calculated as: $\%P_{oS}=100(P_{oC}-P_{o\ max})/P_{oC}$.

SDS PAGE and western blotting

Denaturing gel electrophoresis was performed with a Bio-Rad Mini-Protean Tetra cell, or Life Technologies Bolt Mini Gel system with pre-cast acrylamide gels. Bio-Rad samples were incubated at 60°C for 10 min in 50 mM Tris-HCl, 12.5 mM EDTA, 147 mM β-mercaptoethanol with 2% SDS, 10% glycerol, 0.02% Bromophenol Blue, pH 6.8, then loaded onto a 4-15% TGX gradient gel and run at 200 mV for ∼40 min in 25 mM Tris base, 191 mM Glycine and 0.1% SDS, pH 8.3. Co-IP bound samples were normally loaded onto gels as 5 µl, 10 µl and 15 µl triplicates. Life Technology samples were incubated at 70°C for 10 min in 106 mM Tris-HCl, 141 mM Tris base, 0.51 mM EDTA, 50 mM DTT, 0.22 mM SERVA Blue G250, 0.175 mM Phenol Red with 2% LDS, 10% glycerol (pH 8.5), loaded onto a 4-12% or 10% Bis-Tris Plus gel in 50 mM Tris Base, 50 mM MES, 1 mM EDTA and 0.1% SDS (pH 7.3), then run at 165 mV for ∼50 min, stained with Coomassie Brilliant Blue R-250 or transferred to a 0.45 µm PVDF membrane. Co-IP bound samples were loaded onto the pre-cast acrylamide gels as 10 µl, 15 µl and 20 µl triplicates, or 20 µl added when single sample additions were used. Proteins were transferred in a Mini Trans-Blot module of the Bio-Rad Mini-Protean Tetra cell. In both systems, the PVDF membrane, filter paper and pads used for transfer, were soaked in methanol for 1 min, then cold Transfer buffer (37 mM Tris base, 140 mM glycine, 20% methanol, pH 8.2) for 15 min while rocking. The transfer was performed in Transfer buffer at 100 mV for 60 min, then at 175 mV for 30 min, cooled with an icepack. The post-transfer SDS-PAGE gel was stained with 0.1% (w/v) Coomassie Brilliant Blue R-250 in 5% acetic acid and 20% of ethanol for 1 h with rocking, de-stained overnight in 10% acetic acid and 40% ethanol to determine the efficacy of protein transfer. The efficacy was deemed acceptable if protein bands were absent from the gel.

Immunodetection of RyR, CLIC-2, FKBP12.0 and FKBP12.6

Non-specific antibody binding was prevented by soaking the PVDF membrane in methanol for 1 min, then PBS for 1 min, 3% (w/v) BSA in PBS for 2 h at room temperature (RT), then 0.05% Tween-20 in PBS (TPBS) for 5 min with rocking. The membrane was cut horizontally at 20 kDa and 50 kDa protein standard levels. Upper sections >50 kDa were incubated with 1:4000 of 34c mouse anti-RyR antibody (Developmental Studies Hybridoma Bank, Iowa, USA) in TPBS; middle sections (20-40 kDa) incubated with 1:13,000 'in house' rabbit anti-CLIC2 anti-serum (Board et al., 2004) in TPBS plus 1% (w/v) BSA; lower sections (<20 kDa) incubated with 1:175 mouse anti-FKBP H5 antibody (Santa Cruz Biotechnology, SC133067) in TPBS. In addition, the mouse RyR2 monoclonal antibody (C3-33) used in Fig. S3 was obtained from Abcam (ab2827; 1:1000). After overnight incubation with primary antibodies (∼17 h, at 4°C with rotation), unbound antibodies were removed with 6×5 min washes in ∼40 ml of TPBS and the membrane incubated with secondary antibodies (Santa Cruz Biotechnology) for 2 h at RT; the upper and lower sections incubated with 1:6000 goat anti-mouse IgG-conjugated horseradish peroxidase; the middle section incubated with 1:6000 goat anti-rabbit IgG-conjugated HRP, then TPBS washes repeated to remove unbound secondary antibody. The mouse FKBP monoclonal antibody (H5), anti-mouse IgG peroxidise conjugate and anti-rabbit IgG peroxidise conjugate were obtained from Santa Cruz Biotechnology. An example of reconstructed full western blots following immunostaining of the >20 kDa section with the anti-RyR 34c and the <20 kDa section with anti-FKBP is shown in Fig. S3. These blots were obtained in initial experiments to determine the best antibody for RyR co-IP.

Protein visualisation and densitometric quantification of protein bands

PVDF membranes were coated with chemiluminescent substrate (SuperSignal West Pico Stable Peroxide and Enhancer Solutions) for 2 min and excess substrate removed with a paper towel. The membrane (wrapped in Saran wrap) was placed in a Kodak BioMax Cassette and exposed to light-sensitive film for 30 s to 10 min, depending on signal strength. The film was developed in Kodak dental developer for ≤1 min until protein bands first appeared, then fixed in Kodak dental fixer for 5 min, then rinsed in tap water and allowed to dry. The membrane was exposed to several films for different times, ensuring that all protein bands were suitable for densitometric analysis.

Films were scanned using the GelDoc XR camera (Bio-Rad), and optical density/area of each protein band determined using Quantity One Analysis Software (Bio-Rad). Band densities were analysed within boxes of equal area. Background density in an adjacent area was subtracted from the protein band density. The quantification was carefully designed to avoid signal saturation, with samples loaded as cumulative triplicates. Saturation detected when the band densities of the triplicates did not increase linearly. Protein levels (FKBP and RyR) were quantified only when saturation was absent (see Figs 4 and 7 and Fig. S4). Other criteria were taken into account, including absence of proteins in the final wash samples and an effective protein transfer determined by the post-transfer Coomassie Blue stain. FKBP signal density was expressed relative to the density of the RyR signal in the same lane to avoid errors due to loading volume differences.

Co-sedimentation

Ten µl of SR in 90 µl of buffer containing 20 mM MOPS, 150 mM NaCl, 50 mM sucrose, pH 7.4, plus protease inhibitors (cOmplete, EDTA-free Protease Inhibitor Tablets, Sigma-Aldrich) was incubated for 2 h at 37°C, centrifuged at 100,000 ***g*** for 30 min at 4°C. The pellet was washed three times with MOPS buffer, centrifuging after each wash, then the final pellet washed with 20 µl SDS-PAGE buffer (NuPage LDS sample buffer by Invitrogen) plus 20 µl milliQ water, vortexed, incubated at 70°C for 10 min, 20 µl of sample run on SDS PAGE and transferred for western blotting.

Co-immunoprecipitation

CLIC2 treatment was carried out with ∼400 µg of SR protein solubilised for 15 min on ice in 392 µl IP buffer containing 20 mM MOPS, 150 mM NaCl, 0.01 mM free Ca^{2+} (1 mM $CaCl_2$ plus 91 mM BAPTA), pH 7.0 with 0.1% Triton X-100, 5% glycerol and 8 µl of 50× protease inhibitor cocktail [1 mM benzamidine, 1 mg/l leupeptin, 0.05 mM 4-(2-aminoethyl) benzensulfonyl fluoride hydrochloride, 1 mM pepstatin, anti-calpain I and anti-calpain II]. Solubilized SR was pre-cleared by incubation with non-activated agarose resin for 30 min at RT, incubated with 8 µM CLIC2 for 90 min at RT, then with anti-RyR antibody bound to the coupling aldehyde-activated agarose resin in IP buffer with protease inhibitors for ∼15 h at 4°C. Protein was eluted in 70 µl of 2× SDS-PAGE buffer at 70°C for 10 min, collected by centrifugation at 1000 ***g*** for 1 min, then 10, 15, 20 µl triplicates of sample were run on SDS-PAGE, then transferred for Western blot. Drug treatment with 5 to 20 µM rapamycin (Fig. 7A,B) was performed as for CLIC2. The protocol for Fig. 7E-G was the same except that the IP buffer protease inhibitors were cOmplete, EDTA-free Protease Inhibitor tablets (Sigma-Aldrich), and incubation was for 2 h at RT, with 10 µM rapamycin, 10 µM FK506 or 600 mM NaCl; 20 µl of sample was run on SDS-PAGE, then transferred for western blotting.

Protein cross-linking

Zero length cross-linking was used to covalently stabilise weak or transient interactions via carboxyl-to-amine conjugation using ethyl (dimethylaminopropyl) carbodiimide (EDC) and N-hydroxysuccinimide (NHS) reagents. Crosslinking was performed in MOPS buffer (20 mM MOPS and 150 mM NaCl, pH 7.4) using FKBP isolated from cardiac SR vesicles (Xiao et al., 2007; Galfré et al., 2012). H101Q CLIC-2 protein and/or FKBP in MOPS buffer were incubated at RT for 15 min, then EDC plus NHS added with further 15 min incubation. The reaction was stopped by incubating at 70°C for 10 min with 20 µl of non-reducing sample buffer (106 mM Tris-HCl, 141 mM Tris Base, 2% LDS, 10% glycerol, 0.51 mM EDTA, 0.22 mM SERVA Blue G250 and 0.175 mM Phenol Red, pH 8.5). The incubation time and ratio of cross-linkers were initially optimised for detecting CSQ polymerisation (Wei et al., 2006) with small variations from

Journal of Cell Science

amounts recommended by the manufacturer (Thermo Fisher) in that EDC was added in 45-fold excess of CSQ in the 2006 experiment and EDC in 45-fold excess of CLIC2 was found to be optimal for the present cross-linking experiments. The amounts of FKBP preparation used in the cross-linking experiments was adjusted to give a western blot signal (under conditions identical to the blot processing conditions) that was equivalent to the FKBP12 seen associated with RyR1 in the co-IP experiments (as in Fig. 4). H101Q CLIC2 was added at a concentration of 15 µM, i.e. in 2-4 times greater than that added in the binding/dissociation and channel experiments.

Microscale thermophoresis

Microscale thermophoresis (MST) was carried out according to recommended protocols (User Manual, Monolith NT.115, NanoTemper). CLIC2 was fluorescently labelled as described below and used at a final concentration of 720 nM, which was found in preliminary capillary scans to provide the optimal fluorescence for MST. The total CLIC2 concentration was increased when required by addition of appropriate amounts of unlabelled protein. The equipment allowed scanning of 16 samples per experiment. In each experimental run, one concentration of CLIC2 was assayed against 16 serial dilutions of a potential binding partner (FKBP12 or anti-CLIC2 antibody). The 16 samples were loaded into standard-type MST capillary tubes (NanoTemper) for MST analysis. Temperature-jump and thermophoresis parameters were collected at an MST power of 80% and at a LED power of 20%. Laser duty cycle was 5 s off, 30 s on, 5 s off, with a cool down of 25 s between capillary tubes. For fluorescent labelling, 400 µM Alexa Fluor 647 N-hydroxysuccinimide (NHS) ester (Thermo Fisher) in dimethyl sulfoxide (DMSO) was diluted to 60 µM in PBS, then 100 µl of the Alexa solution added to two separate 100 µl aliquots of 20 µM CLIC2 in PBS. The mixture was incubated for 30 min in the dark. Unreacted free dye was then separated from labelled and unlabelled protein by passing through a gravity-flow purification column (NanoTemper). The eluted sample was assayed for absorbance using a NanoDrop ND-1000 spectrophotometer at both 280 nm and 650 nm in order to determine the relative concentrations of dye and protein and therefore the efficiency of labelling, which was ∼50% with CLIC2. Since fluorescent labelling of FKBP was inefficient (<5%), all experiments were performed with labelled CLIC2. All MST experiments were repeated at least three times.

Statistics

Single-channel data are presented as mean±s.e.m. and significance evaluated by ANOVA using XLSTAT, with multidimensional Mahalanobis test and *post hoc* Fisher analysis. As similar results were obtained at +40 mV and −40 mV in bilayer experiments, data for each potential was included in average data, i.e. two observations for each channel under each condition. To reduce effects of normal variability in the control parameters for RyRs (Copello et al., 1997), open probability with CLIC2 constructs (P_{oT}) is sometimes expressed relative to control open probability (P_{oC}), (i.e. $\log_{10}$ relative $P_o = \log P_{oT} - \log P_{oC}$) as indicated by the relevant axis labels in Fig. 3D,E. For co-IP and co-sedimentation data, significance was assessed either by ANOVA performed using GeneStat or XLSTAT and differences between groups analysed using the Fisher's least significant difference *post hoc* test at a 5% confidence level.

Acknowledgements

The authors are grateful to Ms Suzy Pace and Joan Stivala for their assistance with preparation of SR vesicles from rabbit skeletal muscle and sheep heart. We thank Dr Dan Liu for expressing and purifying the WT and H101Q mutant CLIC2 protein. We also thank Mr Shouvik Aditya for his assistance with fluorescence protein labelling and MST experiments

Competing interests

The authors declare no competing or financial interests.

Author contributions

Conceptualization: S.J.R., G.A.S., N.A.B., A.F.D.; Methodology: S.J.R., G.A.S., E.M.G., P.G.B., M.G.C., N.A.B., A.F.D.; Validation: S.J.R., G.A.S., A.L., M.G.C., N.A.B., A.F.D.; Formal analysis: S.J.R., G.A.S., M.G.C., N.A.B., A.F.D.; Investigation: S.J.R., G.A.S., E.M.G., A.L.; Resources: C.E.S., P.G.B., N.A.B., A.F.D.; Data curation: S.J.R., G.A.S., A.L., M.G.C., N.A.B., A.F.D.; Writing - original draft: S.J.R., G.A.S., A.L., N.A.B., A.F.D.; Writing - review & editing: S.J.R., G.A.S., E.M.G., A.L., C.E.S., P.G.B., M.G.C., N.A.B., A.F.D.; Supervision: M.G.C., N.A.B., A.F.D.; Project administration: P.G.B., N.A.B., A.F.D.; Funding acquisition: P.G.B., N.A.B., A.F.D.

Funding

This work was supported by the National Health and Medical Research Council, Australia [APP008477 to P.G.B. and A.F.D.].

Supplementary information

Supplementary information available online at
http://jcs.biologists.org/lookup/doi/10.1242/jcs.204461.supplemental

References

Ahern, G. P., Junankar, P. R. and Dulhunty, A. F. (1994). Single channel activity of the ryanodine receptor calcium release channel is modulated by FK-506. *FEBS letts.* **352**, 369-374.

Ahern, G. P., Junankar, P. R. and Dulhunty, A. F. (1997). Subconductance states in single-channel activity of skeletal muscle ryanodine receptors after removal of FKBP12. *Biophys. J.* **72**, 146-162.

Aracena, P., Tang, W., Hamilton, S. L. and Hidalgo, C. (2005). Effects of S-glutathionylation and S-nitrosylation on calmodulin binding to triads and FKBP12 binding to type 1 calcium release channels. *Antiox. Redox Signal.* **7**, 870-881.

Beard, N. A., Wei, L., Cheung, S. N., Kimura, T., Varsanyi, M. and Dulhunty, A. F. (2008). Phosphorylation of skeletal muscle calsequestrin enhances its Ca^{2+} binding capacity and promotes its association with junctin. *Cell Calcium* **44**, 363-373.

Bellinger, A. M., Mongillo, M. and Marks, A. R. (2008). Stressed out: the skeletal muscle ryanodine receptor as a target of stress. *J. Clin. Invest.* **118**, 445-453.

Bellinger, A. M., Reiken, S., Carlson, C., Mongillo, M., Liu, X., Rothman, L., Matecki, S., Lacampagne, A. and Marks, A. R. (2009). Hypernitrosylated ryanodine receptor calcium release channels are leaky in dystrophic muscle. *Nat. Med.* **15**, 325-330.

Board, P. G., Coggan, M., Watson, S., Gage, P. W. and Dulhunty, A. F. (2004). CLIC-2 modulates cardiac ryanodine receptor Ca^{2+} release channels. *Int. J. Biochem. Cell Biol.* **36**, 1599-1612.

Chelu, M. G., Danila, C. I., Gilman, C. P. and Hamilton, S. L. (2004). Regulation of ryanodine receptors by FK506 binding proteins. *Trends Cardiovasc. Med.* **14**, 227-234.

Chen, L., Estève, E., Sabatier, J.-M., Ronjat, M., De Waard, M., Allen, P. D. and Pessah, I. N. (2003). Maurocalcine and peptide A stabilize distinct subconductance states of ryanodine receptor type 1, revealing a proportional gating mechanism. *J. Biol. Chem.* **278**, 16095-16106.

Copello, J. A., Barg, S., Onoue, H. and Fleischer, S. (1997). Heterogeneity of Ca^{2+} gating of skeletal muscle and cardiac ryanodine receptors. *Biophys. J.* **73**, 141-156.

Cromer, B. A., Gorman, M. A., Hansen, G., Adams, J. J., Coggan, M., Littler, D. R., Brown, L. J., Mazzanti, M., Breit, S. N., Curmi, P. M. G. et al. (2007). Structure of the Janus protein human CLIC2. *J. Mol. Biol.* **374**, 719-731.

Dulhunty, A. F., Laver, D. R., Gallant, E. M., Casarotto, M. G., Pace, S. M. and Curtis, S. (1999). Activation and inhibition of skeletal RyR channels by a part of the skeletal DHPR II-III loop: effects of DHPR Ser687 and FKBP12. *Biophys. J.* **77**, 189-203.

Dulhunty, A. F., Curtis, S. M., Watson, S., Cengia, L. and Casarotto, M. G. (2004). Multiple actions of imperatoxin A on ryanodine receptors: interactions with the II-III loop "A" fragment. *J. Biol. Chem.* **279**, 11853-11862.

Dulhunty, A. F., Pouliquin, P., Coggan, M., Gage, P. W. and Board, P. G. (2005). A recently identified member of the glutathione transferase structural family modifies cardiac RyR2 substate activity, coupled gating and activation by Ca2+ and ATP. *Biochem. J.* **390**, 333-343.

Dulhunty, A. F., Casarotto, M. G. and Beard, N. A. (2011). The ryanodine receptor: a pivotal Ca^{2+} regulatory protein and potential therapeutic drug target. *Curr. Drug Targets* **12**, 709-723.

Durham, W. J., Aracena-Parks, P., Long, C., Rossi, A. E., Goonasekera, S. A., Boncompagni, S., Galvan, D. L., Gilman, C. P., Baker, M. R., Shirokova, N. et al. (2008). RyR1 S-nitrosylation underlies environmental heat stroke and sudden death in Y522S RyR1 knockin mice. *Cell* **133**, 53-65.

Furuichi, T., Furutama, D., Hakamata, Y., Nakai, J., Takeshima, H. and Mikoshiba, K. (1994). Multiple types of ryanodine receptor/Ca2+ release channels are differentially expressed in rabbit brain. *J. Neurosci.* **14**, 4794-4805.

Galfré, E., Pitt, S. J., Venturi, E., Sitsapesan, M., Zaccai, N. R., Tsaneva-Atanasova, K., O'neill, S. and Sitsapesan, R. (2012). FKBP12 activates the cardiac ryanodine receptor Ca^{2+}-release channel and is antagonised by FKBP12.6. *PLoS ONE* **7**, e31956.

Guo, T., Cornea, R. L., Huke, S., Camors, E., Yang, Y., Picht, E., Fruen, B. R. and Bers, D. M. (2010). Kinetics of FKBP12.6 binding to ryanodine receptors in permeabilized cardiac myocytes and effects on Ca sparks. *Circ. Res.* **106**, 1743-1752.

Györke, S. and Carnes, C. (2008). Dysregulated sarcoplasmic reticulum calcium release: potential pharmacological target in cardiac disease. *Pharmacol. Ther.* **119**, 340-354.
Hewawasam, R., Liu, D., Casarotto, M. G., Dulhunty, A. F. and Board, P. G. (2010). The structure of the C-terminal helical bundle in glutathione transferase M2-2 determines its ability to inhibit the cardiac ryanodine receptor. *Biochem. Pharmacol.* **80**, 381-388.
Jalilian, C., Gallant, E. M., Board, P. G. and Dulhunty, A. F. (2008). Redox potential and the response of cardiac ryanodine receptors to CLIC-2, a member of the glutathione S-transferase structural family. *Antiox. Redox. Signal.* **10**, 1675-1686.
Jeyakumar, L. H., Ballester, L., Cheng, D. S., Mcintyre, J. O., Chang, P., Olivey, H. E., Rollins-Smith, L., Barnett, J. V., Murray, K., Xin, H.-B. et al. (2001). FKBP binding characteristics of cardiac microsomes from diverse vertebrates. *Biochem. Biophys. Res. Commun.* **281**, 979-986.
Jones, J.-L., Reynolds, D. F., Lai, F. A. and Blayney, L. M. (2005). Ryanodine receptor binding to FKBP12 is modulated by channel activation state. *J. Cell. Sci.* **118**, 4613-4619.
Lanner, J. T., Georgiou, D. K., Joshi, A. D. and Hamilton, S. L. (2010). Ryanodine receptors: structure, expression, molecular details, and function in calcium release. *Cold Spring Harb. Perspect. Biol.* **2**, a003996.
Laver, D. R., Eager, K. R., Taoube, L. and Lamb, G. D. (2000). Effects of cytoplasmic and luminal pH on Ca(2+) release channels from rabbit skeletal muscle. *Biophys. J.* **78**, 1835-1851.
Lehnart, S. E., Mongillo, M., Bellinger, A., Lindegger, N., Chen, B. X., Hsueh, W., Reiken, S., Wronska, A., Drew, L. J., Ward, C. W. et al. (2008). Leaky Ca^{2+} release channel/ryanodine receptor 2 causes seizures and sudden cardiac death in mice. *J. Clin. Invest.* **118**, 2230-2245.
Liu, D., Hewawasam, R., Karunasekara, Y., Casarotto, M. G., Dulhunty, A. F. and Board, P. G. (2012a). The inhibitory glutathione transferase M2-2 binding site is located in divergent region 3 of the cardiac ryanodine receptor. *Biochem. Pharmacol.* **83**, 1523-1529.
Liu, X., Betzenhauser, M. J., Reiken, S., Meli, A. C., Xie, W., Chen, B.-X., Arancio, O. and Marks, A. R. (2012b). Role of leaky neuronal ryanodine receptors in stress-induced cognitive dysfunction. *Cell* **150**, 1055-1067.
Mackrill, J. J., O'Driscoll, S., Lai, F. A. and McCarthy, T. V. (2001). Analysis of type 1 ryanodine receptor-12 kDa FK506-binding protein interaction. *Biochem. Biophys. Res. Commun.* **285**, 52-57.
Marx, S. O., Ondrias, K. and Marks, A. R. (1998). Coupled gating between individual skeletal muscle Ca^{2+} release channels (ryanodine receptors). *Science* **281**, 818-821.
Marx, S. O., Reiken, S., Hisamatsu, Y., Jayaraman, T., Burkhoff, D., Rosemblit, N. and Marks, A. R. (2000). PKA phosphorylation dissociates FKBP12.6 from the calcium release channel (ryanodine receptor): defective regulation in failing hearts. *Cell* **101**, 365-376.
Mei, Y., Xu, L., Kramer, H. F., Tomberlin, G. H., Townsend, C. and Meissner, G. (2013). Stabilization of the skeletal muscle ryanodine receptor ion channel-FKBP12 complex by the 1,4-benzothiazepine derivative S107. *PLoS ONE* **8**, e54208.
Meng, X., Wang, G., Viero, C., Wang, Q., Mi, W., Su, X.-D., Wagenknecht, T., Williams, A. J., Liu, Z. and Yin, C.-C. (2009). CLIC2-RyR1 interaction and structural characterization by cryo-electron microscopy. *J. Mol. Biol.* **387**, 320-334.
Noguchi, N., Takasawa, S., Nata, K., Tohgo, A., Kato, I., Ikehata, F., Yonekura, H. and Okamoto, H. (1997). Cyclic ADP-ribose binds to FK506-binding protein 12.6 to release Ca^{2+} from islet microsomes. *J. Biol. Chem.* **272**, 3133-3136.
Oda, T., Yang, Y., Uchinoumi, H., Thomas, D. D., Chen-Izu, Y., Kato, T., Yamamoto, T., Yano, M., Cornea, R. L. and Bers, D. M. (2015). Oxidation of ryanodine receptor (RyR) and calmodulin enhance Ca release and pathologically alter, RyR structure and calmodulin affinity. *J. Mol. Cell. Cardiol.* **85**, 240-248.
Reiken, S., Lacampagne, A., Zhou, H., Kherani, A., Lehnart, S. E., Ward, C., Huang, F., Gaburjakova, M., Gaburjakova, J., Rosemblit, N. et al. (2003). PKA phosphorylation activates the calcium release channel (ryanodine receptor) in skeletal muscle: defective regulation in heart failure. *J. Cell Biol.* **160**, 919-928.
Rullman, E., Andersson, D. C., Melin, M., Reiken, S., Mancini, D. M., Marks, A. R., Lund, L. H. and Gustafsson, T. (2013). Modifications of skeletal muscle ryanodine receptor type 1 and exercise intolerance in heart failure. *J. Heart Lung Transplant.* **32**, 925-929.
Saito, A., Seiler, S., Chu, A. and Fleischer, S. (1984). Preparation and morphology of sarcoplasmic reticulum terminal cisternae from rabbit skeletal muscle. *J. Cell Biol.* **99**, 875-885.
Samarasinghe, K., Liu, D., Tummala, P., Arnolda, L., Casarotto, M. G., Dulhunty, A. F. and Board, P. G. (2015). Glutathione transferase M2 variants inhibit ryanodine receptor function in adult mouse cardiomyocytes. *Biochem. Pharmacol.* **97**, 269-280.
Samsó, M., Shen, X. and Allen, P. D. (2006). Structural characterization of the RyR1-FKBP12 interaction. *J. Mol. Biol.* **356**, 917-927.
Shou, W., Aghdasi, B., Armstrong, D. L., Guo, Q., Bao, S., Charng, M.-J., Mathews, L. M., Schneider, M. D., Hamilton, S. L. and Matzuk, M. M. (1998). Cardiac defects and altered ryanodine receptor function in mice lacking FKBP12. *Nature* **391**, 489-492.
Smith, J. J., Vetter, I., Lewis, R. J., Peigneur, S., Tytgat, J., Lam, A., Gallant, E. M., Beard, N. A., Alewood, P. F. and Dulhunty, A. F. (2013). Multiple actions of phi-LITX-Lw1a on ryanodine receptors reveal a functional link between scorpion DDH and ICK toxins. *Proc. Nat. Acad. Sci. USA* **110**, 8906-8911.
Takano, K., Liu, D., Tarpey, P., Gallant, E., Lam, A., Witham, S., Alexov, E., Chaubey, A., Stevenson, R. E., Schwartz, C. E. et al. (2012). An X-linked channelopathy with cardiomegaly due to a CLIC2 mutation enhancing ryanodine receptor channel activity. *Hum. Mol. Gen.* **21**, 4497-4507.
Timerman, A. P., Ogunbumni, E., Freund, E., Wiederrecht, G., Marks, A. R. and Fleischer, S. (1993). The calcium release channel of sarcoplasmic reticulum is modulated by FK-506-binding protein. Dissociation and reconstitution of FKBP-12 to the calcium release channel of skeletal muscle sarcoplasmic reticulum. *J. Biol. Chem.* **268**, 22992-22999.
Tripathy, A., Resch, W., Xu, L., Valdivia, H. H. and Meissner, G. (1998). Imperatoxin A induces subconductance states in Ca^{2+} release channels (ryanodine receptors) of cardiac and skeletal muscle. *J. Gen. Physiol.* **111**, 679-690.
Wehrens, X. H. T., Lehnart, S. E., Huang, F., Vest, J. A., Reiken, S. R., Mohler, P. J., Sun, J., Guatimosim, S., Song, L.-S., Rosemblit, N. et al. (2003). FKBP12.6 deficiency and defective calcium release channel (ryanodine receptor) function linked to exercise-induced sudden cardiac death. *Cell* **113**, 829-840.
Wehrens, X. H. T., Lehnart, S. E. and Marks, A. R. (2005). Intracellular calcium release and cardiac disease. *Ann. Rev. Physiol.* **67**, 69-98.
Wei, L., Varsányi, M., Dulhunty, A. F. and Beard, N. A. (2006). The conformation of calsequestrin determines its ability to regulate skeletal ryanodine receptors. *Biophys. J.* **91**, 1288-1301.
Wium, E., Dulhunty, A. F. and Beard, N. A. (2012). A skeletal muscle ryanodine receptor interaction domain in triadin. *PLoS ONE* **7**, e43817.
Xiao, J., Tian, X., Jones, P. P., Bolstad, J., Kong, H., Wang, R., Zhang, L., Duff, H. J., Gillis, A. M., Fleischer, S. et al. (2007). Removal of FKBP12.6 does not alter the conductance and activation of the cardiac ryanodine receptor or the susceptibility to stress-induced ventricular arrhythmias. *J. Biol. Chem.* **282**, 34828-34838.
Yan, Z., Bai, X.-C., Yan, C., Wu, J., Li, Z., Xie, T., Peng, W., Yin, C.-C., Li, X., Scheres, S. H. W. et al. (2015). Structure of the rabbit ryanodine receptor RyR1 at near-atomic resolution. *Nature* **517**, 50-55.
Yuan, Q., Deng, K.-Y., Sun, L., Chi, S., Yang, Z., Wang, J., Xin, H.-B., Wang, X. and Ji, G. (2016). Calstabin 2: an important regulator for learning and memory in mice. *Sci. Rep.* **6**, 21087.
Zhang, X., Tallini, Y. N., Chen, Z., Gan, L., Wei, B., Doran, R., Miao, L., Xin, H.-B., Kotlikoff, M. I. and Ji, G. (2009). Dissociation of FKBP12.6 from ryanodine receptor type 2 is regulated by cyclic ADP-ribose but not beta-adrenergic stimulation in mouse cardiomyocytes. *Cardiovasc. Res.* **84**, 253-262.
Zhu, L., Zhong, X., Chen, S. R. W., Banavali, N. and Liu, Z. (2013). Modeling a ryanodine receptor N-terminal domain connecting the central vestibule and the corner clamp region. *J. Biol. Chem.* **288**, 903-914.
Zissimopoulos, S. and Lai, F. A. (2009). FKBP12.6 binding of ryanodine receptors carrying mutations associated with arrhythmogenic cardiac disease. *Biochem. J.* **419**, 273.
Zissimopoulos, S., Docrat, N. and Lai, F. A. (2007). Redox sensitivity of the ryanodine receptor interaction with FK506-binding protein. *J. Biol. Chem.* **282**, 6976-6983.